Theoretical Investigation of Product Channels in the CH_3O_2 + Br Reaction

Joseph S. Francisco*

Department of Chemistry and Department of Earth and Atmospheric Sciences, Purdue University, West Lafayette, Indiana 47907

John N. Crowley

Division of Atmospheric Chemistry, Max-Planck-Institut für Chemie, 55020 Mainz, Germany

Received: November 23, 2005; In Final Form: January 18, 2006

Several reaction pathways on the potential energy surface (PES) for the reaction of CH_3O_2 radicals with Br atoms are examined using both ab initio and density functional methods. Analysis of the PES suggests the presence of the stable intermediates CH_3OOBr and CH_3OBrO. CH_3OOBr is calculated to be more stable than CH_3OBrO by 9.7 kcal mol^{-1} with a significant barrier preventing formation of CH_3OBrO via isomerization of CH_3OOBr. The relative importance of bi- and termolecular product channels resulting from the initially formed CH_3OOBr adduct are assessed based on calculated barriers to the formation of CH_2OO + HBr, CH_3O + BrO, CH_3Br + O_2, and CH_2O + HOBr.

1. Introduction

Bromine species are known to contribute to significant ozone losses both in the polar[1] and midlatitude stratospheres[2] and also in the boundary layer.[3] In a series of measurement campaigns dating back to the late 1980s, tropospheric ozone loss events have been observed in the springtime over the Arctic.[4−6] The cause of these ozone depletion episodes, which typically remove 30−50 ppbv of ozone to levels less than 1 ppbv within a few hours,[7] is thought to be the presence of the reactive bromine compounds, Br and BrO. Recent field measurements by Wingenter et al.[10] revealed elevated levels of methyl bromide (CH_3Br) that coincided with ozone depletion events and which could not be explained by considering its known sources. Wingenter et al.[10] suggested that a minor channel (R1a) in the reaction of methyl peroxy radicals with bromine atoms (R1)

$$CH_3O_2 + Br \rightarrow \text{products} \qquad \text{(R1)}$$

$$CH_3O_2 + Br \rightarrow CH_3Br + O_2 \qquad \text{(R1a)}$$

could be a possible gas-phase source of the enhanced methyl bromide levels, since high levels of Br atoms have been reported at the surface during the Arctic sunrise. According to the calculations of Wingenter et al., in order to generate sufficient CH_3Br to explain the elevated CH_3Br observations, a rate coefficient $k_{1a} = 2.2 \times 10^{-14}$ cm^3 $molecule^{-1}$ s^{-1} would be needed. Only one laboratory study of the CH_3O_2 radical reaction with bromine atoms has been reported to date.[11] Aranda et al.[11] studied the reaction of CH_3O_2 + Br in a discharge flow mass spectrometer/laser-induced fluorescence (LIF) setup. By directly monitoring the pseudo-first-order loss rate of CH_3O_2 radicals in an excess of Br atoms, they determined $k_1 = 4.4 \times 10^{-13}$ cm^3 $molecule^{-1}$ s^{-1} at 298 K. The possible exothermic and thermoneutral bimolecular product channels discussed by Aranda et al.[11] involved the formation of CH_3O + BrO or HBr + CH_2O_2. The formation of CH_3Br (R1a), as suggested by Wingenter[10] is also thermodynamically possible as is the formation of CH_2O + HOBr.

$$CH_3O_2 + Br \rightarrow CH_3Br + O_2 \qquad \text{(1a)}$$

$$\rightarrow CH_2OO + HBr \qquad \text{(1b)}$$

$$\rightarrow CH_3O + BrO \qquad \text{(1c)}$$

$$\rightarrow CH_2O + HOBr \qquad \text{(1d)}$$

On the basis of the observation and quantification of an ion signal at $m/z = 95$, coincident with the parent ion of BrO, Aranda et al.[11] concluded that channel R1c was the dominant, if not the sole, reaction pathway, with a branching ratio of 0.8−1.0 at 298 K. They were unable to observe the CH_3O coproduct using LIF and invoked its removal by reaction with the excess reactant Br to explain this. This reaction has a room-temperature rate constant[14] of 7×10^{-11} cm^3 $molecule^{-1}$ s^{-1} and is expected to result in the formation of HBr (the only exothermic bimolecular reaction possible).

$$CH_3O + Br \rightarrow HBr + CH_2O \qquad (2)$$

Aranda et al.[11] report however that HBr was not observed as a product in their experiments. This observation not only rules out a significant contribution of R1b but appears to be inconsistent with the explanation for nondetection of CH_3O and thus casts doubt on the suggestion that channel 1c is dominant. They do not report the measurement of CH_3Br or any signals at other masses. In addition to the bimolecular reaction pathways listed above, it is also conceivable that a termolecular channel forming stabilized CH_3OOBr may exist. Indeed, several investigations of the reactions of the peroxy radicals $C_2H_5O_2$, $BrC_2H_4O_2$, and $HOC_2H_4O_2$ with Br atoms[15] and also peroxy radicals with I atoms[16] strongly suggest that ROOX (where X = Br or I) is formed at significant yield and with a large rate constant at the pressures involved in those experiments (200−

* To whom correspondence should be addressed. E-mail: francisc@purdue.edu.

10.1021/jp056794r CCC: $33.50
Published on Web 02/10/2006

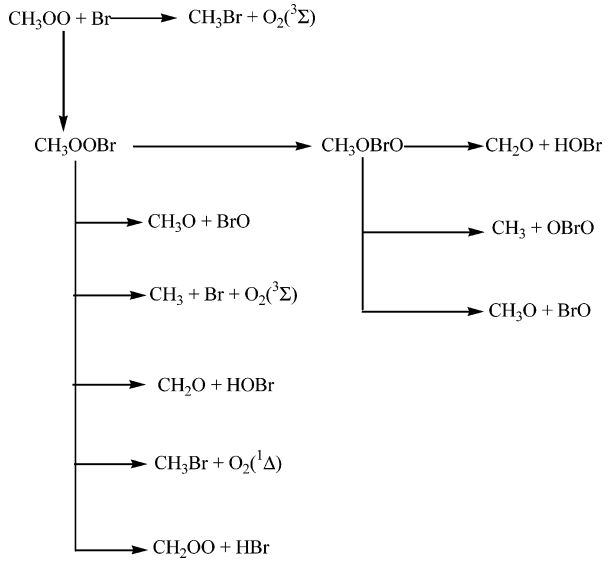

Figure 1. CH_3OO + Br reaction scheme.

760 Torr of air or N_2). There are two potential explanations why Aranda et al.[11] do not report the observation of CH_3OOBr in their studies. The most obvious is that this termolecular process is not favored under the experimental conditions of their experiment, where the total pressure was only 1 Torr of He. Alternatively, it is unlikely that CH_3OOBr would have a stable positive ion at its parent mass to enable its unambiguous detection by mass spectrometry (previous experiments have utilized absorption spectroscopy to detect ROOBr). Indeed, CH_3OOBr would most likely fragment to form BrO^+ at a mass of 95, which would complicate the interpretation of the origin of this mass and indeed preclude its definite assignment to the BrO radical. A third reason for the nondetection of CH_3OOBr is related to its chemical stability in their system and is discussed later.

The goal of this study is thus to explore the potential energy surface of the Br + CH_3O_2 reaction in order to provide insight into the formation of intermediates and products.

2. Computational Methods

The calculations in this study were performed with the GAUSSIAN03 program.[17] Preliminary searches of global minima and transition states were carried out using the unrestricted second-order Møller−Plesset perturbation theory (MP2) method[18] and using the density functional method with the hybrid B3LYP functional.[19] Results from these calculations were used to search for the global minima transition states by the quadratic configuration interaction with the singles and doubles method (QCISD).[20] With the MP2, B3LYP, and QCISD methods, the 6-31G(d) basis set was used in the optimizations. Geometry optimizations were carried out for all structures using Schlegel's method[21] to better than 0.001 Å for bond lengths and 0.01° for angles, with a self-consistent field convergence of at least 10^{-9} on the density matrix. The residual rms (root-mean-square) force is less than 10^{-4} au. Vibrational frequency calculations using the B3LYP/6-31G(d) method were performed to verify whether the structure had either all positive frequencies (minima) or one imaginary frequency (a first-order saddle point). To improve the energetics, fixed-point calculations were performed with several higher order methods, the spin projected fourth-order Møller−Plesset perturbation method (PMP4),[22] the coupled cluster method using singles, doubles, and perturbation correction for the triples [CCSD(T)] method,[23] and the quadratic configuration interaction method with singles, doubles, and perturbative corrections for the triples [QCISD(T)] method. These calculations were performed with the 6-311++G(2df,2p) basis set. Because spin contamination can produce inaccurate total energies when performing these calculations, they were closely monitored. The $\langle s^2 \rangle$ value showed no significant signs that there were major deviations from the expected $\langle s^2 \rangle$ value of 0.75 for open shell species.

TABLE 1: Heats of Formation for Key Species Involved in the CH_3O_2 + Br Reaction

	ΔH_0° (kcal mol^{-1})
Br	28.2 ± 0.0[a]
BrO	30.2 ± 1[a]
CH_2O	-25.1 ± 1.5[b]
HOBr	-10.93 ± 1[c]
HBr	-6.8 ± 1[a]
CH_3	35.8 ± 0.2[a]
CH_3Br	-8.96 ± 0.36[d]
CH_3OO	8.0 ± 1[e]

[a] Chase, M. W.; Davies, C. A.; Dawners, J. R.; Friup, D. J.; McDonald, R. A.; Syverad, A. N. *J. Phys. Chem. Ref. Data* **1985**, *1*. [b] Curtiss, L. A.; Raghavachari, K.; Redfern, P. C.; Pople, J. A. *J. Chem. Phys.* **1997**, *106*, 1063. [c] Lock, M.; Barnes, R. J.; Sinha, A. *J. Phys. Chem.* **1996**, *100*, 7972. [d] Fowell, P.; Lancher, J. R.; Park, J. D. *Trans. Faraday Soc.* **1965**, *61*, 1324. [e] Using the D_o of 86.9 ± 1.0 from CH_3OO-H from Blanksby, S. J.; Ramond, T. M.; Davies, G. E.; Nimlos, M. R.; Kato, S.; Bierbaum, V. M.; Lineberger, W. C.; Ellison, G. B.; Okumura, M. *J. Am. Chem. Soc.* **2001**, *123*, 9685 and using the heat of formation of CH_3OOH from ref 25.

TABLE 2: Energetics Calibration

	$\Delta H_{r,o}^\circ$		
reaction	calcd	exp	$\lvert\Delta\rvert$
$CH_3OO + Br \rightarrow CH_2O + HOBr$	−71.5	−72.2	0.7
$CH_3OO + Br \rightarrow CH_3Br + O_2(^3\Sigma)$	−42.1	−45.2	3.1
$CH_3OO + Br \rightarrow CH_3 + Br + O_2(^3\Sigma)$	27.4	27.8	0.4

3. Results and Discussion

As discussed in the Introduction, the only reported product of the CH_3O_2 + Br reaction is BrO, formed in a slightly endothermic reaction pathway (R1c). Figure 1 outlines various reaction channels and indicates two pathways that can lead to BrO, both involving passage through either the CH_3OOBr or CH_3OBrO intermediates. The CH_3OOBr complex initially formed can either directly dissociate to BrO + CH_3O via O atom transfer or isomerize through a three-center bromine migration to form CH_3OBrO, which can also decompose by an O−Br bond fission to BrO and CH_3O. The other product channels which are accessible from CH_3OOBr or CH_3OBrO require significant rearrangement.

In the following, we calculate the energetics for the various reaction channels listed in Figure 1. Beforehand, to evaluate whether the levels of theory used are reasonable, the energetics for several possible reactions involved in the CH_3OO + Br system, for which there is accurate experimental thermochemical data from the literature (Table 1), are used to test the methodology. In Table 2, the calculated heats of reaction represent the geometric average of results calculated at the CCSD(T)/6-311++G(2df,2p)//B3LYP/6-31G(d) and the QCISD(T)/6-311++G(2df,2p)//QCISD/ 6-31G(d) levels of theory. A comparison between calculated and experimental energetics show that the rms error in the energetics is ±2.2 kcal mol^{-1}. In fact, a reexamination of the energetics for reaction 1c, using the CCSD(T) and QCISD(T) averaged results, shows that the heat of reaction is 4.5 kcal mol^{-1} and is consistent with the estimate

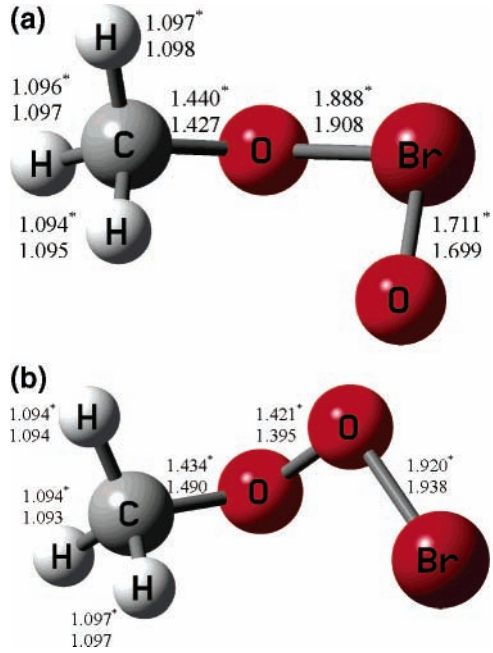

Figure 2. Structure of the CH_3OOBr and CH_3OBrO intermediates. Numbers without an asterisk are calculated at the B3LYP/6-31G(d) level of theory, and the numbers with an asterisk are calculated at the QCISD/6-31G(d) level of theory.

of 5 ± 3 kcal mol^{-1} from Aranda et al.[11] Nevertheless, the averaged CCSD(T) and QCISD(T) energetics are reasonable and can provide some useful insight into the mechanism for the CH_3O_2 + Br reaction.

As mentioned above, the relative importance of the various product channels of the Br + CH_3O_2 reaction will depend on the energies of the intermediates CH_3OOBr and CH_3OBrO and the barrier heights for their rearrangement to end-products. These intermediates are described theoretically in this paper (Figure 2). The transition states for the various reaction pathways in the CH_3O_2 + Br reaction are given in Figure 3, the heats of reaction and transition state barriers are given in Table 3, and a PES is displayed in Figure 4.

The CH_3OOBr and CH_3OBrO intermediates are both thermodynamically very stable, being 27.4 and 16.3 kcal mol^{-1} lower in energy than the reactants, respectively. Papayannis et al.[24] calculated the stability difference between CH_3OBrO and CH_3OOBr to be 6.3 kcal mol^{-1} at the G2MP2 level of theory. Our result is consistent with that obtained by Papayannis et al.[24] The 9.7 kcal mol^{-1} difference in energy of the two intermediates is consistent with the difference of 8.4 kcal mol^{-1} found for CH_3OClO and CH_3OOCl.[25] It is also interesting to compare CH_3OOBr to CH_3OOH, for which the O−O bond energy[26] is 43.2 kcal mol^{-1}, suggesting that CH_3OOBr is somewhat less stable than CH_3OOH.

The barrier for isomerization of CH_3OOBr to CH_3OBrO is 67.3 kcal mol^{-1} at the CCSD(T)/6-311+G(2df,2p)//B3LYP/6-31G(d) level of theory. This isomerization passes through a three-center transition state, shown in Figure 3a, that involves a bromine migration to the carbon-bonded oxygen atom. This transition state is similar to that found for CH_3OOCl[25] and CH_3OOI.[27] For these systems and CH_3OOBr, the transition state exhibits triangular geometries as seen by Drougas and Kosmas.[24,25,27] The isomerization barrier of 43.1 kcal mol^{-1} is above the CH_3O_2 + Br reactant level, suggesting that the formation of CH_3OBrO is inefficient. If any CH_3OBrO is formed by the isomerization process, then it will readily isomerize via a small barrier of 6.6 kcal mol^{-1} through a five-center transition state, shown in Figure 3b, to produce CH_2O + HOBr. We touch on this later when we make comparisons with the isoelectronic reaction of CH_3O + BrO.

Having established that the reaction of CH_3O_2 + Br favors the formation of the CH_3OOBr intermediate, we now consider the fate of this complex in terms of stabilization or rearrangement into various bimolecular product channels.

Formation of CH_3O + BrO. The simple dissociation of the CH_3OOBr complex via Br−O bond fission to make BrO + CH_3O proceeds with a barrier of 33.2 kcal mol^{-1}. The occurrence of this reaction channel appears at first to be supported by the experimental work of Aranda et al.,[11] who report observation of the BrO product (but not CH_3O). This channel is 2.9 kcal mol^{-1} above the CH_3O_2 + Br reactants, and the rate of production of CH_3O + BrO should be slow at room temperature. This appears to be consistent with the low rate constant for this process reported by Aranda et al.[11]

Formation of CH_2OO + HBr. The barrier to formation of CH_3O + BrO (R1c) is slightly higher than the barrier of 30.3 kcal mol^{-1} for the rearrangement to CH_2OO + HBr (R1b), which thus turns out to theoretically be the most feasible bimolecular product channel if the calculations for the formation enthalpy of the Criegee radical, CH_2OO, are correct. This can be compared to the results obtained by Schnell et al.[28] on the CH_3O + ClO reaction. They show that the CH_3OOCl passes through a five-center transition that involves the Cl abstracting the hydrogen from the methyl group. A similar five-center transition state is found for the CH_3OOBr adduct and is shown in Figure 3c. The carbon−hydrogen bond on the methyl group that is being abstracted is elongated by 1.277 D, slightly larger than the 1.215 D reported in the chlorine analogue. The H−Br distance is found to be 1.767 D compared to 1.438 D in molecular HBr. The barrier for CH_3OOBr going to CH_2OO + HBr is 30.3 kcal mol^{-1}, which compares well to the barrier of 27.0 kcal mol^{-1} reported by Papayannis et al.[24] It is also consistent with the barrier calculated by Schnell et al.[28] of 30.8 kcal mol^{-1} for the CH_3OOCl reaction producing CH_2O_2 + HCl. These predictions are however not commensurate with the nondetection of the HBr product in the experimental study of Aranda et al.[11] We note that the formation of the CH_2OO coproduct would probably remain undetected in a chemical system with excess bromine atoms, as a fast reaction to form BrO + CH_2O would be expected.

$$CH_2OO + Br \rightarrow CH_2O + BrO \qquad (3)$$

Other bimolecular product channels accessible from the CH_3OOBr complex are CH_3 + Br + O_2, CH_2O + HOBr, and CH_3Br + O_2. The formation of CH_3 + Br + O_2 is endothermic by ≈54 kcal mol^{-1} (see Figure 4), and the formation of these products from CH_3OOBr dissociation need not be further considered.

Formation of CH_2O + HOBr. Of the remaining possibilities, channel R1d (formation of CH_2O and HOBr) represents the most exothermic reaction channel. This reaction passes through a four-center transition state in which the hydrogen from the carbon of the methyl group forms on O−H bond with oxygen connected to the Br of CH_3OOBr (Figure 3d). In the transition state, the C−H and the O−O bonds in CH_3OOBr break while the OH bond is formed and the C−O single bond hybridizes to a C=O double bond while forming CH_2O. The barrier is above the CH_3OOBr intermediate by 35.6 kcal mol^{-1}. Note that this transition state is 8.2 kcal mol^{-1} above the reactants CH_3O_2 + Br. The G2MP2 calculations of Papayannis et al.[24] suggest this barrier to be 3.8 kcal mol^{-1} above the reactants. In their experimental

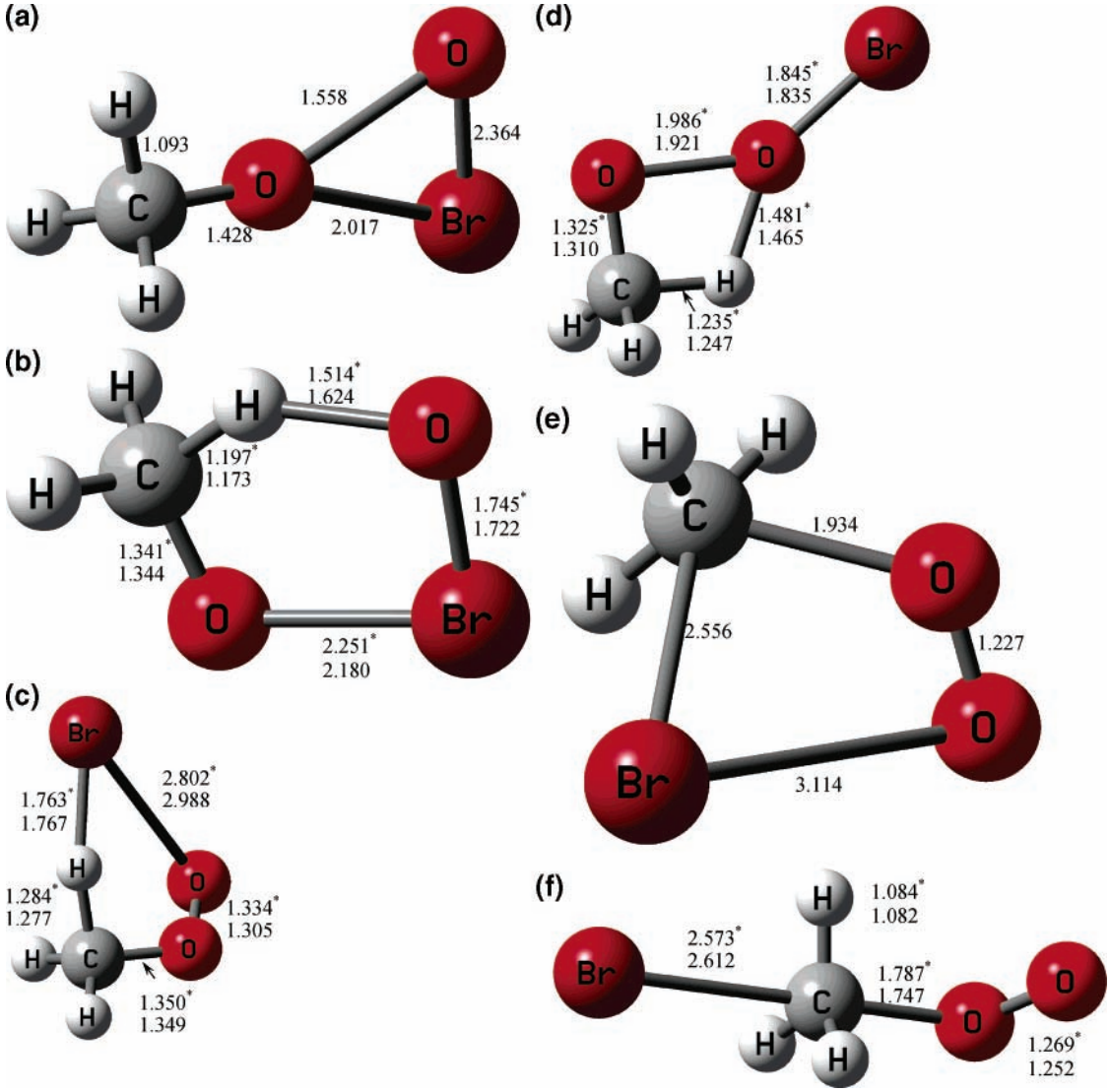

Figure 3. Transition state structures for reaction pathways inovlved in the CH_3OO + Br reaction. Numbers without an asterisk are calculated at the B3LYP/6-31G(d) level of theory, and the numbers with asterisk are calculated at the QCISD/6-31G(d) level of theory: (a) $CH_3OOBr \rightarrow CH_3OBrO$ (TS1), (b) $CH_3OBrO \rightarrow CH_2O + HOBr$ (TS2), (c) $CH_3OOBr \rightarrow CH_2OO + HBr$ (TS3), (d) $CH_3OOBr \rightarrow CH_2O + HOBr$ (TS4), (e) $CH_3OOBr \rightarrow CH_3Br + O_2(^1\Delta)$ (TS5), and (f) $CH_3OO + Br \rightarrow CH_2Br + O_2(^3\Sigma)$ (TS6).

study, Aranda et al.[11] do not report detection of HOBr (which they have detected on other occasions),[29] and we can probably rule this out as a major reaction pathway.

Formation of $CH_3Br + O_2$. One of the initial goals of this study was to investigate whether CH_3Br can be formed from the title reaction. One pathway that can produce CH_3Br from CH_3OOBr is via the formation of $O_2(^1\Delta)$ on the CH_3OOBr singlet surface. The transition state shown in Figure 3e passes through a four-center transition state, which involves breaking the Br−O bond while forming the C−Br bond and the C−O bond breaks while the O−O forms a double bond. The O−O bond length is 1.227 D, and it is apparent that the transition state for this process is rather late as evidenced by the elongated Br−O bond of 3.114 D and the nearly broken C−O bond at 1.934 D. The activation energy barrier for this process is estimated to be 88.5 kcal mol^{-1} at the CCSD(T)/ 6-311++G-(2df,2p)//B3LYP/6-31G(d) level of theory. It is clear that this cannot be a significant source of CH_3Br. However, because the CH_3O_2 + Br reaction involves a reaction between two doublet spin state species, the reaction can occur on both the singlet and triplet surfaces.

On the triplet surface, there are two processes that can occur for the CH_3O_2 + Br reaction. One involves the formation of CH_3OOBr (^3A) in the triplet state followed by the dissociation of CH_3OOBr (^3A) into $CH_3Br + O_2$ ($^3\Sigma$) through a four-center transition state similar to that shown in Figure 3e. The CH_3-$OOBr$ (^3A) species is located about 21.4 kcal mol^{-1} above the CH_3OOBr (^1A), placing it 6.0 kcal mol^{-1} below the CH_3O_2 + Br reactants. The barrier for the dissociation of CH_3OOBr (^3A) into $CH_3Br + O_2$ ($^3\Sigma$) passing through a four-center transition state is estimated to be 44.7 kcal mol^{-1} at the PMP4/6-311++G-(2df,2p) level of theory and as such is not a major route for forming $CH_3Br + O_2$ ($^3\Sigma$). However, there is an interesting unexpected route to the formation of $CH_3Br + O_2$ ($^3\Sigma$) that is more competitive. The transition state for this reaction is shown in Figure 3f. The Br approaches the C of the CH_3O_2 radical while the C−O bond starts to break. The approach of the Br is collinear with the C−O bond, such that the BrCO angle is 180.0°. The barrier for this reaction with respect to the CH_3O_2 + Br reactants is 10.9 kcal mol^{-1}. This channel is competitive with the dissociation of CH_3OOBr (^1A) into CH_2O + HOBr on the singlet surface. The $CH_3Br + O_2$ ($^3\Sigma$) channel on the triplet

TABLE 3: Energetics for Reaction Pathways Involved in the CH_3O_2 + Br Reaction

	$CH_3OO + Br \rightarrow CH_3Br + O_2(^3\Delta)$		$CH_3OOBr \rightarrow CH_2O + HOBr$		$CH_3OOBr \rightarrow CH_2OO + HBr$		$CH_3OOBr \rightarrow CH_3Br + O_2(^1\Delta)$	
method	$\Delta H_{r,o}°$	barrier	$\Delta H_{r,o}°$	barrier	$\Delta H_{r,o}°$	barrier	$\Delta H_{r,o}°$	barrier
B3LYP/6-31G(d)	−41.7	2.6	−34.6	38.8	18.8	31.4	23.7	80.1
PMP4/6-311++G(2df,2p)	−44.9	17.7	47.4	31.4	13.2	24.3	14.1	86.6
CCSD(T)/6-311++G(2df,2p)	−40.0	15.2	−47.1	35.7	11.2	30.0	14.2	88.5
QCISD/6-31G(d)	−59.3	−3.2	−42.1	45.9	13.3	40.6	14.0	
QCISD(T)/6-311++G(2df,2p)	−44.1	6.6	−43.5	35.4	10.9	30.7	19.1	
Avg.[a]	−42.1	10.9	−45.3	35.6	11.1	30.3	16.6	

	$CH_3OOBr \rightarrow CH_3OBrO$		$CH_3OBrO \rightarrow CH_2O + HOBr$		$CH_3OBrO \rightarrow CH_3 + OBrO$	$CH_3OBrO \rightarrow CH_3O + BrO$	$CH_3O + Br \rightarrow CH_3O + BrO$	$CH_3OOBr \rightarrow CH_3OO + Br$	$CH_3OOBr \rightarrow CH_3O + BrO$	$CH_3OOBr \rightarrow CH3 + Br + O_2(^3\Sigma)$
method	$\Delta H_{r,o}°$	barrier	$\Delta H_{r,o}°$	barrier	$\Delta H_{r,o}°$	$\Delta H_{r,o}°$	$\Delta H_{r,o}°$	$\Delta H_{r,o}°$	$\Delta H_{r,o}°$	$\Delta H_{r,o}°$
B3LYP/6-31G(d)	18.7	68.7	−53.4	2.6	61.9	11.3	3.8	26.2	30.1	55.9
PMP4/6-311++G(2df,2p)	7.9	66.3	−55.2	1.9	52.1	26.6	7.1	27.4	34.5	50.9
CCSD(T)/6-311++G(2df,2p)	10.0	67.3	−57.2	6.2	58.0	19.1	4.9	24.2	29.1	52.6
QCISD/6-31G(d)	19.9		−62.0	8.6	63.0	6.0	−13.7	39.7	26.6	46.1
QCISD(T)/6-311++G(2df,2p)	9.4		−52.9	6.9	65.3	26.9	4.0	33.1	37.2	61.5
Avg.[a]	9.7		−55.1	6.6	61.7	23.0	4.5	26.2	33.2	53.8

[a] The geometric average of CCSD(T)/6-311++G(2df,2p) and QCISD(T)/6-311++G(2df,2p) data.

surface may represent a minor product channel for the CH_3O_2 + Br reaction.

Formation of CH_3OOBr in a Termolecular Channel. A further possibility is that the CH_3OOBr association complex can be stabilized by collisions to be the final product in a termolecular process as discussed in the Introduction. This is somewhat akin to the self-reaction of ClO, which proceeds via formation of a ClOOCl complex which can be stabilized at low temperatures[30] but which dissociates into three bimolecular product channels at ambient temperature.[31] The formation of CH_3OOBr in a barrierless association of CH_3O_2 and Br is thus favored by high pressures which collisionally deactivate the complex and prevent dissociation back to the reactants. The low reactivity of CH_3O_2 toward Br compared to the fast reactions of, for example, $BrC_2H_4O_2$ or $C_2H_5O_2$ with Br reflects the reduced number of vibrational degrees of freedom on CH_3O_2 compared to the larger peroxy radicals, but most importantly, it reflects the vastly different experimental conditions under which the experiments were carried out (1 Torr of He for CH_3O_2 + Br vs 200−600 Torr of N_2/air for RO_2 + Br in the studies of Crowley and Moortgat[15,31]).

Comparison with the Isoelectronic Reaction CH_3O + BrO. It is interesting to compare the CH_3O_2 + Br reaction with the CH_3O + BrO reaction (R4). From an electronic structure perspective, these two reactions are isoelectronic, yet from a reactivity perspective, they are rather different. Aranda et al.[11] have determined a rate constant of $(3.8 \pm 0.4) \times 10^{-11}$ cm^3 molecule^{-1} s^{-1} for (R4)

$$CH_3O + BrO \rightarrow \text{products} \qquad (4)$$

which is about a factor of 100 faster than the CH_3O_2 + Br reaction. By analogy to the reaction of CH_3O with ClO, which has a similar rate room-temperature constant ($(2.3 \pm 0.3) \times 10^{-11}$ cm^3 molecule^{-1} s^{-1})[32] and forms CH_2O and HOCl, the most likely products of R4 are CH_2O and HOBr.

These products cannot be obtained readily from the CH_3OOBr adduct because a much larger (35.6 kcal mol^{-1}) barrier passing through a four-center transition state (Figure 3d) has to be overcome. On the other hand, the CH_3O + BrO reaction can proceed via direct formation of the CH_3OBrO intermediate, which can undergo a five-centered hydrogen transfer reaction (Figure 3b), in which a much smaller 6.6 kcal mol^{-1} barrier from CH_3OBrO must be overcome to produce the products CH_2O + HOBr. Since the exogernicity in producing CH_3OBrO from CH_3O + BrO is 25.3 kcal mol^{-1}, the highly energized CH_3OBrO adduct will dissociate to produce the CH_2O + HOBr products. This energetic picture of the CH_3O + BrO reaction is supported by the work of Papayannis et al.[24] The difference in rate coefficient and products of these two reactions is thus readily explained by the possibility of CH_3O + BrO to form CH_3OBrO, which is apparently not available for CH_3O_2 + BrO.

Can we reconcile the theoretical calculations on CH_3O_2 + Br with the experimental results of Aranda et al.?[11] Let us first assume that BrO + CH_3O is the major (or sole) product channel of the title reaction as reported by Aranda et al.[11] The rather low rate constant for this process at room temperature (k_1 = 4.4×10^{-13} cm^3 molecule^{-1} s^{-1}) is then consistent with a reaction that passes through a transition state that is slightly higher in energy than the reactants. The difference between the low rate constant observed for CH_3O_2 + Br compared to other peroxy radicals could then be a result of an inefficient termolecular channel forming stabilized CH_3OOBr at 1 Torr of He (see above). On the other hand, we note that, even if CH_3OOBr were thermalized at 1 Torr of He, it would probably have a rather short lifetime in the presence of an excess of Br atoms in the reactor. The products of CH_3OOBr + Br are likely to be Br_2 + CH_3O_2[15]

$$CH_3OOBr + Br \rightarrow CH_3O_2 + Br_2 \qquad (5)$$

As the CH_3O_2 radical is reformed in this process, this channel is not measured experimentally and the reported value of k_1 is in fact a lower limit that may represent only a fraction of the overall rate constant. The Br_2 coproduct of R5 would also not be observable experimentally, as large concentrations of Br_2 are used to generate the Br reactant.

A second possibility, already mentioned above, is that the m/z = 95 signal is in fact partly or wholly due to an ion fragment of CH_3OOBr. The authors report that the m/z = 95 ion signal

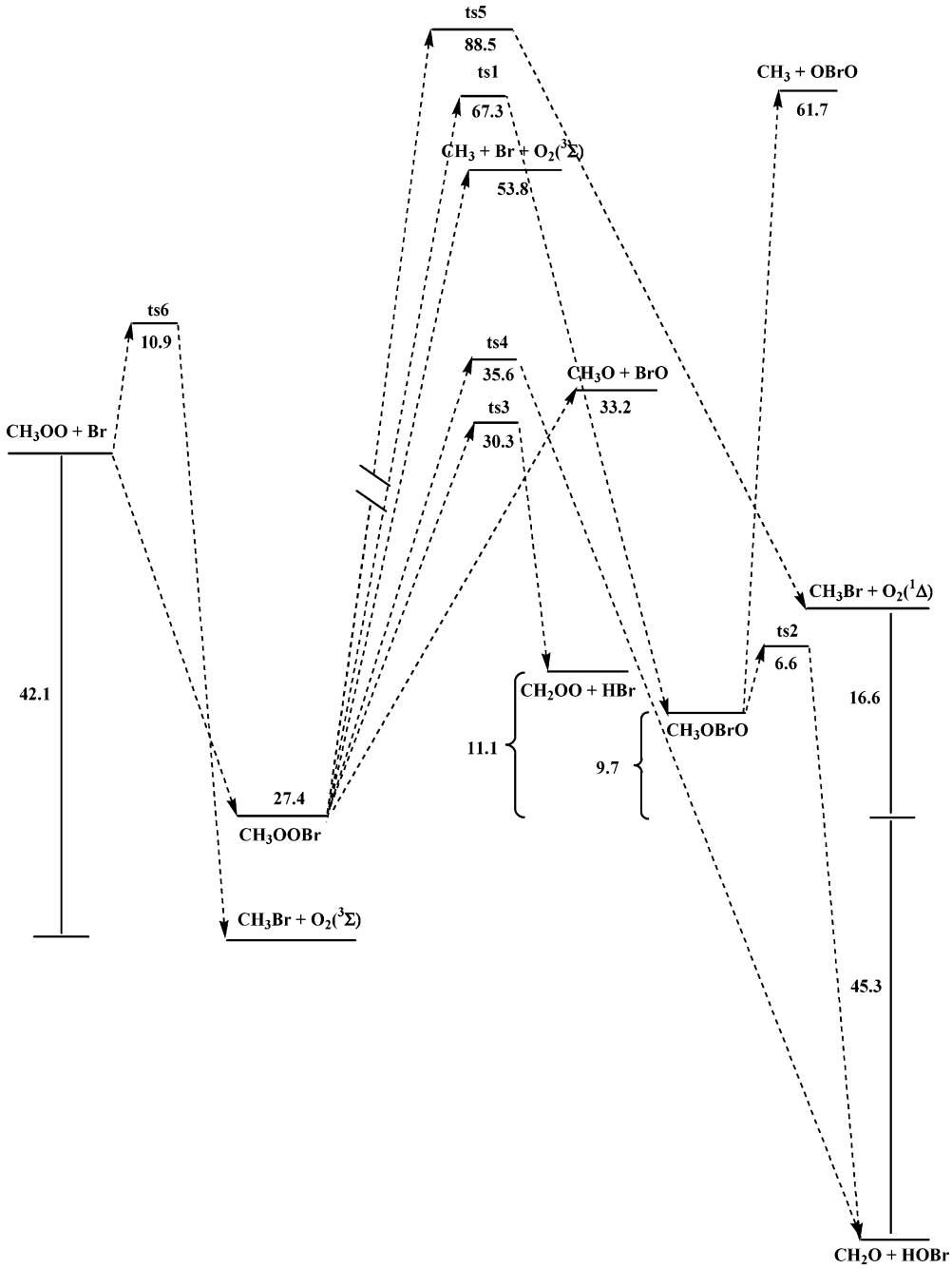

Figure 4. Potential energy surface for the CH_3OO + Br reaction. Numbers are given in units of kcal mol^{-1}.

they assigned to BrO grows with reaction time but do not report the kinetics of this process, which may be influenced by the presence of other radicals (e.g., CH_3O). The same discussion could equally well apply to CH_3OOBr, which likely would react with Br (see above). The ionization cross section of CH_3OOBr is unlikely to be vastly different from that of BrO, and similar signals at $m/z = 95$ may be expected.

Elucidation of the true mechanism and overall rate constant for this reaction under atmospheric conditions requires further experimental studies. Especially, the temperature and pressure dependence of the reaction would give us valuable information on the role of intermediates and the competition between the bi- and termolecular reaction pathways.

4. Conclusion

We have investigated pathways for the reaction of CH_3O_2 radicals with Br atoms. This theoretical study suggests that the CH_3O_2 + Br reaction is dominated by the formation of the CH_3OOBr intermediate, the formation of which is calculated to be without a barrier. Bimolecular reaction pathways via CH_3OOBr dissociation (in order of most favored first) are CH_2OO + HBr, CH_3O + BrO, and CH_2O + HOBr, which is not consistent with the experimentally reported dominance of a single reaction channel forming BrO.

Another minor bimolecular product channel is the direct formation of CH_3Br + O_2 ($^3\Sigma$) in an S_N2 displacement of O_2 from the CH_3O_2 + Br reaction which occurs on the triplet surface. The finding of this minor channel raises the question of whether the CH_3Br + O_2 ($^3\Sigma$) reaction could be a possible contributing source of CH_3Br. Nevertheless, the dominate channel is however the termolecular CH_3OOBr forming channel which is consistent with the previous experimental studies of RO_2 + Br that did not consider R═CH_3. These results suggest that new laboratory measurements on the products and kinetics

of the reaction of Br + CH_3O_2 are desirable, as is a reassessment of the potential role of this reaction in the bromine chemistry of the lower and free troposphere.

Acknowledgment. We thank Oliver Wingenter for stimulating this research in discussions about the potential role of the title reaction as an atmospheric source of CH_3Br. We would like to thank the Jet Propulsion Laboratory at the California Institute of Technology for providing generous support of supercomputer time. The Cray supercomputer was provided by funding from NASA of the Mission to Planet Earth, Aeronautics, and Space Science.

References and Notes

(1) Solomon, S. *Nature* **1990**, *347*, 347.
(2) Daniel, J. S.; Soloman, S.; Partmann, R. W.; Garcia, R. R. *J. Geophys. Res*. **1999**, *105*, 23871.
(3) von Glasow, R.; von Kuhlmann, R.; Lawrence, M. G.; Platt, U.; Crutzen, P. *J. Atmos. Chem. Phys.* **2004**, *4*, 2481.
(4) Barrie, L. A.; Bottenheim, J. W.; Schnell, R. C.; Crutzen, P. J.; Rasmussen, R. A. *Nature* **1988**, *334*, 134.
(5) Bottenheim, J. W.; Barrie, L. A.; Atlas, E.; Heidt, L. E.; Niki, H.; Rasmussen, R. A.; Shepson, P. B. *J. Geophys. Res*. **1990**, *93* (D11), 18555.
(6) Hausmann, M.; Platt, U. *J. Geophys. Res*. **1994**, *99* (D12), 25399.
(7) Yokouchi, Y.; Toom-Sauntry, D.; Yazawa, K.; Inagaki, T.; Tamaru, T. *Atmos. Environ.* **2002**, *36*, 4985.
(8) Salawich, R. J.; McElroy, M. B.; Yatteau, J. H.; Wofsy, S. C.; Schoeberl, M. R.; Lait, L. R.; Newman, P. A.; Chan, K. R.; Loewenstein, M.; Podolske, J. R.; Strahan, S. E.; Profitt, M. H. *Geophys. Res. Lett.* **1990**, *17*, 561.
(9) Barrie, L. A.; Li, S. M.; Toom, D. L.; Bandsberger, S.; Sturges, W. *J. Geophys. Res*. **1994**, *99*, 25453.
(10) Wingenter, D. W.; Sive, B. C.; Blake, D. R.; Rowland, F. S.; Ridley, B. A. *Geophys. Res. Lett*. **2003**, *30*, 2160.
(11) Aranda, A.; Laverdet, G.; LeBras, G.; Poulet, G. *J. Chim. Phys*. **1998**, *95*, 963.
(12) Kafafi, S. A.; Martinez, R. I.; Herran, J. T. *Molecular Structure and Energetics*; Lieman, J. F., Greenbers, A., Eds.; VCH Publishers: Deerfield Beach, FL, 1987.
(13) Sander, S. P.; et al. *Evaluation Number 14 JPL Publication 02-25*; Jet Propulsion Laboratory, California Institute of Technology: Pasadena, CA, 2003.
(14) Aranda, A.; Daële, V.; LeBras, G.; Poulet, G. *Int. J. Chem. Kinet*. **1998**, *30*, 249.
(15) Crowley, J. N.; Moortgat, G. K. *J. Chem. Soc., Faraday Trans*. **1992**, *88*, 2437.
(16) Jenkin, M. E.; Cox, R. A. *J. Phys. Chem.* **1991**, *95*, 3229.
(17) Frisch, M. J.; Trucks, G. W.; Schlegel, H. B.; Scuseria, G. E.; Robb, M. A.; Cheeseman, J. R.; Montgomery, J. A., Jr.; Vreven, T.; Kudin, K. N.; Burant, J. C.; Millam, J. M.; Iyengar, S. S.; Tomasi, J.; Barone, V.; Mennucci, B.; Cossi, M.; Scalmani, G.; Rega, N.; Petersson, G. A.; Nakatsuji, H.; Hada, M.; Ehara, M.; Toyota, K.; Fukuda, R.; Hasegawa, J.; Ishida, M.; Nakajima, T.; Honda, Y.; Kitao, O.; Nakai, H.; Klene, M.; Li, X.; Knox, J. E.; Hratchian, H. P.; Cross, J. B.; Bakken, V.; Adamo, C.; Jaramillo, J.; Gomperts, R.; Stratmann, R. E.; Yazyev, O.; Austin, A. J.; Cammi, R.; Pomelli, C.; Ochterski, J. W.; Ayala, P. Y.; Morokuma, K.; Voth, G. A.; Salvador, P.; Dannenberg, J. J.; Zakrzewski, V. G.; Dapprich, S.; Daniels, A. D.; Strain, M. C.; Farkas, O.; Malick, D. K.; Rabuck, A. D.; Raghavachari, K.; Foresman, J. B.; Ortiz, J. V.; Cui, Q.; Baboul, A. G.; Clifford, S.; Cioslowski, J.; Stefanov, B. B.; Liu, G.; Liashenko, A.; Piskorz, P.; Komaromi, I.; Martin, R. L.; Fox, D. J.; Keith, T.; Al-Laham, M. A.; Peng, C. Y.; Nanayakkara, A.; Challacombe, M.; Gill, P. M. W.; Johnson, B.; Chen, W.; Wong, M. W.; Gonzalez, C.; Pople, J. A. *Gaussian 03*, revision C.02; Gaussian, Inc.: Wallingford, CT, 2004.
(18) Møller, C.; Plesset, M. S. *Phys. Rev*. **1934**, *46*, 618.
(19) Becke, A. M. *J. Chem. Phys*. **1993**, *98*, 5648.
(20) Pople, J. A.; Head-Gordon, M.; Raghavachari, K. *J. Chem. Phys*. **1987**, *87*, 5968.
(21) Schlegel, H. B. *J. Comput. Chem*. **1982**, *3*, 214.
(22) Schlegel, H. B. *J. Chem. Phys*. **1986**, *84*, 4530.
(23) Raghavachari, K.; Trucks, G. W.; Pople, J. A.; Head-Gordon, M. *Chem. Phys. Lett*. **1989**, *157*, 479.
(24) Papayannis, D. K.; Melissas, V. S.; Kosmas, A. M. *Phys. Chem. Chem. Phys.* **2003**, *5*, 2976.
(25) Drougas, E.; Kosmas, A. M. *Int. J. Quantum Chem*. **2004**, *98*, 335.
(26) Matthews, J.; Sinha, A.; Francisco, J. S. *J. Chem. Phys*. **2005**, *122*, 221101.
(27) Drougas, E.; Kosmas, A. M. *Can. J. Chem.* **2005**, *83*, 9.
(28) Schnell, M.; Muhlhauser, M.; Peyerimhoff, S. D. *J. Phys. Chem. A* **2004**, *108*, 1298.
(29) Bedjanian, Y.; Riffault, V.; Poulet, G. *J. Phys. Chem. A* **2001**, *105*, 3167.
(30) Bloss, W. L.; Nickolaisen, S. L.; Salewitch, R. L.; Friedl, R. R.; Sander, S. P. *J. Phys. Chem*. **2001**, *105*, 11226.
(31) Horowitz, A.; Crowley, J. N.; Moortgat, G. K. *J. Phys. Chem*. **1994**, *98*, 11924.
(32) Daele, V.; Laverdet, G.; Poulet, G. *Int. J. Chem. Kinet*. **1996**, *28*, 589.